THE JOURNAL OF PHYSICAL CHEMISTRY B LETTERS

2008, *112,* 4854−4858
Published on Web 03/28/2008

Interactions and Dynamics in Ionic Liquids

Alexander Stoppa, Johannes Hunger, and Richard Buchner*

Institut für Physikalische und Theoretische Chemie, Universität Regensburg, D-93040 Regensburg, Germany

Glenn Hefter

Chemistry−DSE, Murdoch University, Murdoch, W.A. 6150, Australia

Andreas Thoman and Hanspeter Helm

Department of Molecular and Optical Physics, Albert-Ludwigs-Universität Freiburg, D-79104 Freiburg, Germany

Received: January 29, 2008; In Final Form: February 29, 2008

Precise dielectric spectra have been determined at 25 °C over the exceptionally broad frequency range of 0.1 $\leq \nu$/GHz $\leq$ 3000 for the imidazolium-based room-temperature ionic liquids (RTILs) [bmim][BF_4], [bmim][PF_6], [bmim][DCA], and [hmim][BF_4]. The spectra are dominated by a low-frequency process at ∼1 GHz with a broad relaxation time distribution of the Cole−Davidson or Cole−Cole type, which is thought to correspond to the rotational diffusion of the dipolar cations. In addition, these RTILs possess two Debye relaxations at ∼5 GHz and ∼0.6 THz and a damped harmonic oscillation at ∼2.5 THz. The two higher-frequency modes are almost certainly due to cation librations, but the origin of the ∼5 GHz mode remains obscure.

Introduction

Room-temperature ionic liquids (RTILs) are attracting intense interest because of their unusual properties and potentially vast range of applications in chemical synthesis, industrial processing, and energy storage.[1,2] It is clear from the physicochemical characteristics of RTILs (electrical conductivity, viscosity, etc.) that they differ from conventional organic solvents. However, they are also not just simple mixtures of ions nor are their properties necessarily closely analogous to those of traditional high-temperature molten salts.[3] However, little is known about the nature and the interactions of the species present in RTILs, and even less is known about their dynamic behavior. This lack of understanding inhibits the rational development and exploitation of this exciting new class of materials.

The properties of RTILs are undoubtedly dominated by the inherently strong, long-range Coulombic interactions among the ions. Although progress has been made in computational studies, the size and flexibility of most RTILs, as well as the complexity of the interactions among proximate cations and anions, still present significant problems.[4−6] Such interactions are also difficult to probe by the usual spectroscopic techniques (NMR, IR, etc.), which are mostly sensitive to localized effects and by conventional thermodynamic or transport measurements that are insufficiently species sensitive. In contrast, being responsive to dipolar species, the frequency-dependent dielectric function, $\hat{\epsilon}(\nu)$, provides direct access to molecular-level interactions and dynamics over very wide ranges of molecular size and time scales.[7] Broadband dielectric spectroscopy (DS) is, however, technologically challenging as several types of purpose-built equipment and sophisticated signal processing techniques are required to cover the whole spectrum.[7,8] Thus, virtually all dielectric spectra of RTILs to date have been restricted to either low ($\nu \lesssim 20$ GHz)[9−12] or high ($\nu \gtrsim 500$ GHz)[13−15] frequencies. Only recently, the intermediate frequency region was covered for the pyrrolidinium salt [$p_{1,2}$][DCA], revealing considerable excess absorption above ∼50 GHz.[16] While such spectra have yielded many useful insights, they have not provided a comprehensive picture of the liquid-state dynamics of RTILs and indeed may even be misleading with respect to various aspects of the nature of RTILs.

Proper characterization of $\hat{\epsilon}(\nu)$ is of major concern for our understanding of solvation phenomena in RTILs, especially the underlying dynamical aspects, as the time-dependent response of the solvent to solute-induced perturbations controls ultrafast reactions, especially charge-transfer processes.[17−19] It is well-known that solvation dynamics in polar liquids is essentially determined by the frequency-dependent dielectric function of the solvent and can be described within the framework of dielectric continuum models.[20] However, recent application of this approach to solvation dynamics in RTILs was not successful.[17,18] It was found that a considerable part of the short-time dynamics was missed by the continuum models used. Currently, it cannot be determined whether the discrepancy between the experimentally observed solvation dynamics in RTILs and the predictions based on dielectric continuum models results from an insufficient frequency coverage of the published $\hat{\epsilon}(\nu)$ or a breakdown of the applied dielectric continuum models. Clearly,

* To whom correspondence should be addressed. E-mail: richard.buchner@chemie.uni-regensburg.de

10.1021/jp800852z CCC: $40.75

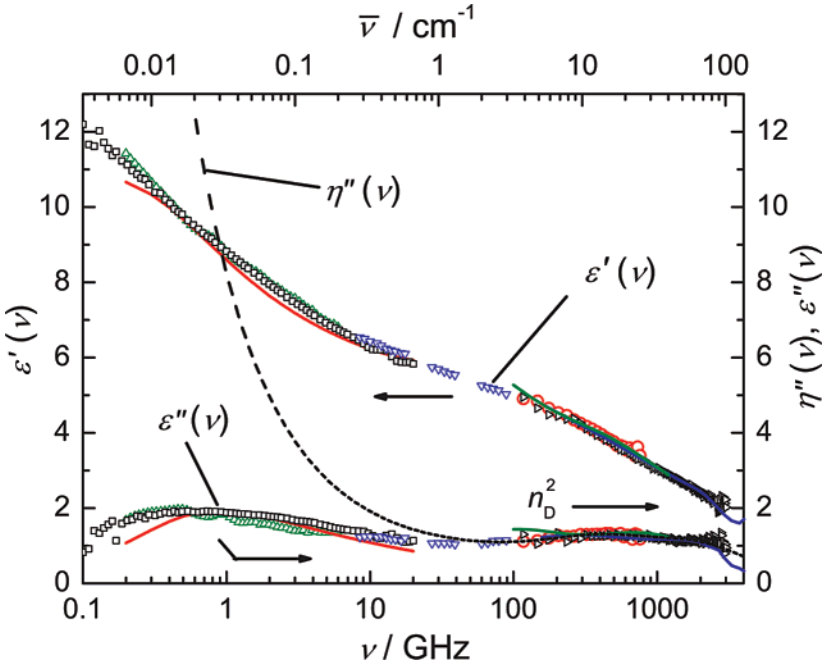

Figure 1. Experimental permittivity, $\epsilon'(\nu)$, and dielectric loss, $\epsilon''(\nu)$, of [bmim][BF_4] in the microwave and far-infrared regions obtained with VNA, black □; TDR, green △; IFMs, blue ▽; THz-TDS transmission, red ○; and THz-TDS reflection, black right-pointing triangle, spectrometer. For comparison, the smoothed data of Schroeder et al.[11] (red line), Yamamoto et al.[14] (blue line), and Koeberg et al.[15] (green line) are included. The dashed line shows the total loss, $\eta''(\nu) = \epsilon''(\nu) + \kappa/(2\pi\nu\epsilon_0)$, of the sample; n_D is the refractive index at the Na−D line.

only precise $\hat{\epsilon}(\nu)$ data covering a frequency range as large as possible can end this stalemate.

Accordingly, this paper presents dielectric spectra of several imidazolium-based RTILs over virtually the entire useful dielectric frequency range, $0.1 \lesssim \nu/\text{GHz} \lesssim 3000$. Imidazolium salts were chosen for study because they have been widely adopted as "representative" RTILs and are readily synthesized and purified.

Materials and Methods

The RTILs selected for study were 1-*N*-butyl-3-*N*-methylimidazolium tetrafluoroborate, [bmim][BF_4], and its hexafluorophosphate, [bmim][PF_6], and dicyanamide, [bmim][DCA], analogues, as well as 1-*N*-hexyl-3-*N*-methylimidazolium tetrafluoroborate, [hmim][BF_4]. These compounds were prepared from purified reactants[22,23] and dried under vacuum ($p < 10^{-8}$ bar) at ~40 °C, yielding water contents < 40ppm and halide impurities of <150 ppm, <20 ppm, <0.5%, and <20 ppm, respectively. These highly hygroscopic liquids were stored in a nitrogen-filled glovebox, and the measurements were conducted under a dry N_2 atmosphere.

Broadband dielectric spectra were obtained by a combination of data from a time domain reflectometer (TDR), $0.2 \le \nu/\text{GHz} \le 6$,[24] a frequency domain reflectometer based on a vector network analyzer (VNA) at $0.1 \lesssim \nu/\text{GHz} < 20$,[25] four waveguide interferometers (IFMs) at $8.5 \le \nu/\text{GHz} \le 89$,[26] and a transmission/reflection THz time domain spectrometer (THz-TDS) at $0.3 \le \nu/\text{THz} \le 3$.[27,28] All measurements were conducted at (25.00 ± 0.05) °C, except for the THz-TDS spectra which were recorded at (25.0 ± 0.5 °C). Raw VNA data were corrected for calibration errors with a Padé approximation.[29]

Results and Discussion

The quantity measured in DS is the total complex dielectric response, $\hat{\eta}(\nu)$, which is related to the complex permittivity $\hat{\epsilon}(\nu)$ via the equation

$$\hat{\eta}(\nu) = \hat{\epsilon}(\nu) - \frac{i\kappa}{2\pi\nu\epsilon_0} = \epsilon'(\nu) - i\left(\epsilon''(\nu) + \frac{\kappa}{2\pi\nu\epsilon_0}\right) \quad (1)$$

where $\epsilon'(\nu)$ and $\epsilon''(\nu)$ are, respectively, the frequency-dependent permittivity and dielectric loss, κ is the dc conductivity, and ϵ_0 is the permittivity of free space. As previously,[25] κ was treated as an adjustable parameter, but the values so obtained were always close to those determined by conventional means. The accessible minimum frequency of our spectra ($\nu_{min} \approx 0.1$ GHz) is determined by the threshold $\epsilon''(\nu_{min})/\Delta\eta''(\nu_{min}) < 1$ since the experimentally obtained total loss, $\eta''(\nu) = \epsilon''(\nu) + \kappa/(2\pi\nu\epsilon_0)$, and its error, $\Delta\eta''(\nu_{min})$, strongly increase with decreasing frequency, whereas $\epsilon''(\nu)$ decreases.

The excellent concordance among the present $\hat{\epsilon}(\nu)$ data for [bmim][BF_4] is shown in Figure 1. Comparable results were obtained for the other RTILs. The overlap of $\epsilon'(\nu)$ and $\epsilon''(\nu)$ values produced by the IFMs with those from the TDR and VNA, which only yield data relative to a permittivity standard, shows that the calibration procedures for the latter two instruments were reliable. The present spectra for [bmim][BF_4] also agree well with the limited literature data available in the MW[11] and THz regions,[14,15] albeit with discrepancies at the low- and high-frequency edges (Figure 1). Almost certainly, these differences reflect the larger experimental uncertainties of all data sources at their low- and high-frequency limits.

All of the present spectra (Figures 1 and 2) show broad peaks in $\epsilon''(\nu)$ in the low GHz and THz regions and a reasonably distinct plateau in $\epsilon'(\nu)$ at around 20−80 GHz. These spectra clearly demonstrate that extrapolation to $\nu = 0$ of THz data alone to obtain the static permittivity or dielectric constant

$$\epsilon_s = \lim_{\nu \to 0} \epsilon'(\nu)$$

as done by several authors,[13,15] is not reliable because of the presence of processes in the MW region. Similarly, it is unwise to infer the nature of the fast dynamics of RTILs on the basis

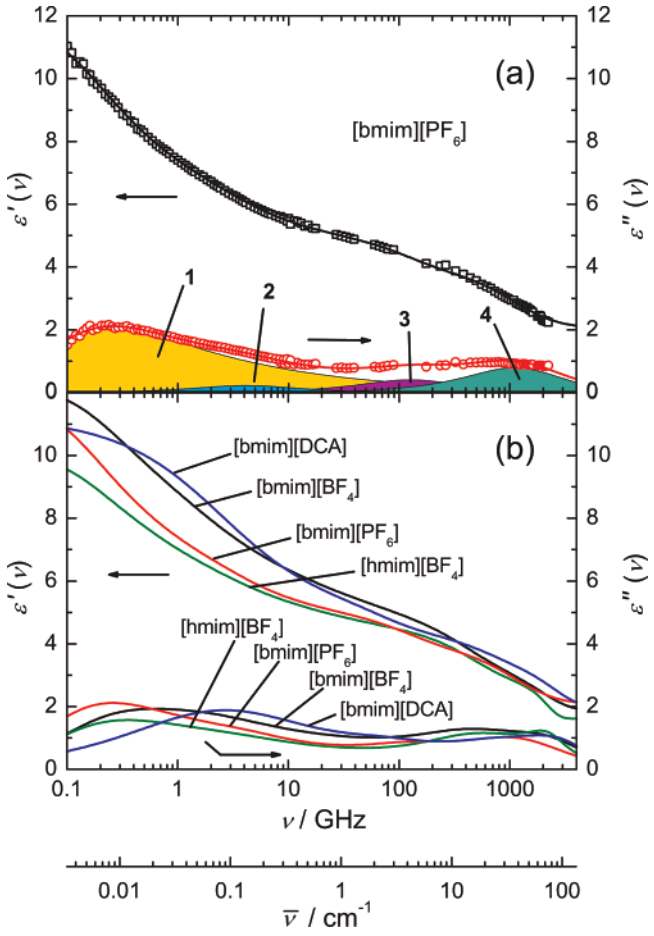

Figure 2. (a) Permittivity, $\epsilon'(\nu)$, and dielectric loss, $\epsilon''(\nu)$, spectra (symbols) of [bmim][PF_6], together with the fit (lines) of the CD + D + D + DHO model. Shaded areas indicate the contributions of the individual processes j ($j = 1...4$) of eq 2 to $\epsilon''(\nu)$. (b) Smoothed spectra of the investigated RTILs calculated with the parameters of Table 1.

of measurements at $\nu \lesssim 20$ GHz. Like *N*-methyl-*N*-ethylpyrrolidinium dicyanamide,[16] all of the present imidazolium RTILs exhibit a marked loss contribution at high frequencies, which produces a minimum in $\epsilon''(\nu)$ at around 50 GHz (Figures 1 and 2).

To find the best formal description of $\hat{\epsilon}(\nu)$, conceivable relaxation models of the type

$$\hat{\epsilon}(\nu) = \sum_{j=1}^{n} S_j \tilde{F}_j(\nu)$$

were tested by assuming $2 \le n \le 6$ possible individual contributions j of amplitude S_j and band-shape function $\tilde{F}_j$. The selection criterion among the various tested models was the value of the reduced error function, χ_r^2. Details of the fitting procedure are given elsewhere.[32] For all samples, a combination of four processes ($n = 4$) yielded the best fit (smallest χ_r^2). The slowest mode, $j = 1$, centered at ~1 GHz, had a broad relaxation time distribution. The shape of this distribution is of the Cole−Davidson (CD) type, with shape parameters $\alpha_1 = 0$ and $0 < \beta_1 < 1$, for the highly viscous [bmim][BF_4], [bmim][PF_6], and [hmim][BF_4], or of the Cole−Cole (CC) type (at a slightly higher frequency), with $0 < \alpha_1 < 1$ and $\beta_1 = 1$, for the less viscous [bmim][DCA]. In addition, there were two Debye (D) relaxations at ~5 GHz ($j = 2$) and ~0.6 THz ($j = 3$) and a damped harmonic oscillator (DHO) contribution ($j = 4$) centered around 2−3 THz. Combination of these processes gives the overall fitting equation

$$\hat{\epsilon}(\nu) = \epsilon_\infty + \frac{S_1}{(1 + (i2\pi\nu\tau_1)^{1-\alpha_1})^{\beta_1}} + \frac{S_2}{1 + i2\pi\nu\tau_2} + \frac{S_3}{1 + i2\pi\nu\tau_3} + \frac{S_4\nu_4^2}{\nu_4^2 - \nu^2 + i\gamma_4\nu} \quad (2)$$

where τ_j is the relaxation time and $\nu_j = {}^1/_2\pi\tau_j$ the peak frequency of process $j = 1, ..., 3$; ν_4 is the resonance frequency, and γ_4 and the damping constant, of the DHO contribution, and

$$\epsilon_\infty = \lim_{\nu\to\infty} \epsilon'(\nu)$$

is the infinite frequency permittivity. The fit parameters obtained are summarized in Table 1.

TABLE 1: Fit Parameters of Equation 2 and the Corresponding Reduced Error Function, χ_r^2, for Present RTILs at 25 °C[a]

ionic liquid	[bmim][BF_4]	[bmim][PF_6]	[bmim][DCA]	[hmim][BF_4]
ϵ_s	12.2 ± 1.4	11.8 ± 0.7	11.3 ± 1.0	10.1 ± 1.3
S_1	8.94	7.04	6.42	6.32
τ_1	1140	1406	63.0	1322
α_1	0	0	0.33	0
β_1	0.21	0.37	1	0.27
S_2	0.37	0.45	0.75	0.18
τ_2	73.1	38.8	2.09	42.6
S_3	1.15	0.81	0.94	1.46
τ_3	0.389	1.26	0.240	0.331
S_4	0.70	1.38	1.04	0.69
ν_4	2.85	2.77	3.68	2.4[b]
γ_4	4.85	7.77	6.37	2.47
ϵ_∞	1.06	2.10	2.13	1.47
n_D^2	2.0155 [c]	1.9850 [c]		2.0270[d]
$10^3\chi_r^2$	2.2	2.5	0.9	2.1

[a] For convenience, the static dielectric constant, $\epsilon_s = \epsilon_\infty + \sum S_j$, and its estimated extrapolation error, as well as literature data of the squared refractive index at the sodium D line, n_D^2, are also tabulated. Units: τ_1, τ_2, and τ_3 in 10^{-12} s; ν_4 and γ_4 in THz. [b] Parameter fixed during the fit procedure. [c] Ref 30. [d] Ref 31.

RTIL Dynamics. Dielectric spectroscopy monitors the fluctuations of the total dipole moment in a sample and thus is a direct probe for RTIL dynamics. Such fluctuations correspond to "molecular" reorientations, librations, and intermolecular vibrations which occur on femto- to nanosecond time scales.

Typical for many viscous liquids,[7] the dielectric spectra of [bmim][BF_4] (viscosity $\eta \approx 0.14$ Pa s[33−37]), [bmim][PF_6] ($\eta \approx 0.31$ Pa s[34,37−39]), and [hmim][BF_4] ($\eta = 0.24$ Pa s[40]) are dominated by a highly nonexponential low-frequency relaxation ($j = 1$ in eq 2) with a loss peak centered at 0.3−1 GHz that can be accounted for by a strongly asymmetric CD relaxation time distribution. The small β_1 values (Table 1) suggest a highly inhomogeneous "molecular" environment for the relaxing dipoles. On the other hand, for the less viscous [bmim][DCA] ($\eta = 0.033$ Pa s[40]), the same mode, centered at ~3 GHz, exhibits a symmetrical CC broadening. Weingärtner et al.[12] have suggested that this low-frequency relaxation of RTILs is dominated by reorientation of dipolar cations (the present anions have small (DCA) or zero (BF_4^-, PF_6^-) dipole moments). This interpretation is supported by the proportionality (Figure 3) of the average relaxation time of this mode, $\tau_1^{av} = 1/(2\pi\nu_{max})$, to η. The ν_{max} is the peak frequency of the calculated $\epsilon''(\nu)$ for relaxation $j = 1$ (mode 1). According to the Stokes−Einstein−

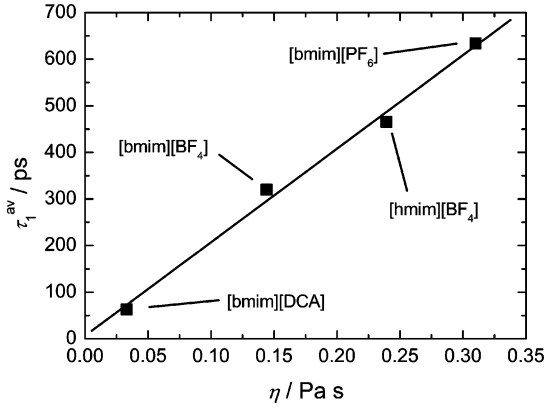

Figure 3. Average relaxation time, τ_1^{av}, of the lowest-frequency relaxation ($j = 1$ in eq 2) as a function of RTIL viscosity, η.

Debye relation, $\tau \propto \eta$ is expected for rotational diffusion of individual molecular dipoles as the underlying relaxation mechanism. However, it must be noted that the correlation in Figure 3 might be fortuitous because the η values for [bmim][BF_4] and [bmim][PF_6] have abnormally large uncertainties.[33−39]

All of the present RTILs show a small-amplitude relaxation ($j = 2$ in eq 2) at ∼5 GHz (Table 1 and Figure 2a). A similar process was observed by Weingärtner et al.,[10−12] but because of their more limited frequency range, the values of Weingärtner et al. for τ_2 (and τ_1) are generally smaller than those in Table 1. While anion rotation may contribute to mode 2 for [bmim][DCA], this cannot explain the observation of mode 2 for the RTILs with the nonpolar BF_4^- and PF_6^- anions. Despite its small amplitude, the reality of relaxation $j = 2$ (mode 2) is supported by the presence of a mode, with a similar time constant, in optical heterodyne-detected Raman-induced Kerr effect spectra (OHD-RIKES).[41] The latter was attributed to a "correlated bulk motion in the salt",[41] but the precise origin of process 2 remains obscure. On the other hand, the relaxation times reported by the Quitevis group[42−44] for the slow OHD-RIKES component of their investigated RTILs are intermediate to our τ_2 and τ_3 (Table 1). Note that these authors[42−44] refrain from an interpretation of their slow mode due to an insufficient signal-to-noise ratio.

The minimum in $\epsilon''(\nu)$ at ∼50 GHz and its broad peak in the THz region for the present RTILs cannot be fitted with a single process. Previous THz studies invoked either two[13,15] or (with due reservation) three[14] Debye relaxations to fit the spectra in this region. Giraud et al.[41] used a sum of six Brownian oscillators to fit their OHD-RIKES between ∼30 GHz and ∼6 THz. Hyun et al.[42] combined two low-frequency Lorentzians with a Bucaro−Litovitz and an antisymmetrized Gaussian (ASG) line shape function to fit their OHD-RIKES spectra in a similar frequency range, whereas Xiao et al.[44] added two further ASGs to describe the intermolecular dynamics. In contrast, the present spectra at $\nu > 100$ GHz were well fit with a Debye relaxation ($j = 3$ in eq 2) centered at ∼700 GHz and a damped harmonic oscillator (DHO, $j = 4$) at ∼2.5 THz (Table 1). The noise level at $\nu \gtrsim 2.5$ THz is too large to distinguish between D and DHO processes, but the latter is preferred for the fastest mode because librations or intermolecular vibrations would be expected to dominate at such high frequencies.[41] This interpretation is consistent with the observation that $\epsilon_\infty \lesssim n_D^2$ in the present spectra (Figure 1) and by the shape of the spectra of Yamamoto et al.[14] at $\nu > 3$ THz, which exhibit a pronounced minimum in $\epsilon'(\nu)$ indicative of a resonance contribution.

Giraud et al. suggest that their OHD-RIKES bands at approximately 30, 65, and 100 cm^{-1} (∼0.9, 2, and 3 THz) correspond to out-of-plane librations of the cation with the closest counterion at different positions with respect to the imidazolium ring.[41] A similar assignment was given by Xiao et al. to their OHD-RIKES bands at approximately 30, 60, 100, and 170 cm^{-1} (∼0.9, 1.8, 3 and 5 THz).[44] It is therefore likely that both high-frequency modes 3 and 4 of the present spectra can be assigned to cation librations. However, it must be noted that the number of THz bands reported in the OHD-RIKES[41−44] and the previous THz studies,[13−15] as well as their positions and amplitudes, differ considerably among each other and from those of Table 1.

Static Permittivity. It is important to note that DS provides the only way of directly measuring the static permittivity (dielectric constant, $\epsilon_s = \epsilon_\infty + \sum S_j$), for RTILs since traditional capacitance methods cannot be used for conducting liquids. The present values of ϵ_s for [bmim][BF_4] and [bmim][PF_6] are in good agreement with those obtained by Weingärtner et al.[9,11] from their dielectric spectra recorded at $0.2 \leq \nu/\text{GHz} \leq 20$. The larger than usual uncertainties in ϵ_s occur because $\epsilon'(\nu)$ has not yet reached a plateau at the lowest experimentally accessible frequencies (Figure 2). On the other hand, the values of $\epsilon_s \approx 7$ reported for imidazolium RTILs from THz studies[13,15] are clearly underestimates as they neglect the significant MW contribution to $\hat{\epsilon}(\nu)$. The result of $\epsilon_s = 68.89$ reported by Wu and Stark[45] for [bmim][BF_4] from low-frequency impedance measurements is not realistic. Such a value could only be obtained if there was an additional dispersion step with a relaxation time of ∼50−100 ns. Although dielectric measurements in this region are swamped by the conductivity contribution (Figure 1 and eq 1), given the typically broad nature of dielectric absorbances, the presence of such a process should be easily discernible in the present spectra. Furthermore, Weingärtner et al.[12] have shown that static permittivities of ∼8−15 for imidazolium RTILs are compatible with the number densities and dipole moments of the constituent ions. Our analysis of $\epsilon - \epsilon_\infty$ yields similar results.

Concluding Remarks

Although the uncertainties are not optimal, the controversial question[9,11,13,15,45] of the static permittivity of RTILs can now be considered settled; depending on the dipole moments of their constituent ions, imidazolium RTILs have ϵ_s values of 10−25.[9] For the investigated salts, the now available formal description of the dielectric function between 0.1 GHz and ∼3 THz, given by eq 2 and the parameters of Table 1, should be sufficient to crosscheck the dielectric continuum models for RTIL solvation dynamics. However, the situation with regard to RTIL dynamics is still unsatisfactory. While our spectra agree well with previous, more limited, investigations and provide a self-consistent link between the MW and THz regions, a coherent formal description of dielectric and OHD-RIKES spectra and a molecular interpretation in terms of specific dynamic processes in RTILs remain the major challenge for understanding this important class of liquids.

Acknowledgment. The authors thank W. Kunz for access to his laboratory facilities. This work was funded by the Deutsche Forschungsgemeinschaft within Priority Program 1191.

References and Notes

(1) Wasserscheid, P., Welton, T., Eds. *Ionic Liquids in Synthesis*; Wiley-VCH: Weinheim, Germany, 2003.
(2) Parvulescu, V. I.; Hardacre, C. *Chem. Rev.* **2007**, *107*, 2615.
(3) Dupont, J. *J. Braz. Chem. Soc.* **2004**, *15*, 341.

(4) Urahata, S. M.; Ribeiro, M. C. C. *J. Chem. Phys.* **2004**, *120*, 1855.
(5) Wang, Y.; Voth, G. *J. Am. Chem. Soc.* **2005**, *127*, 12192.
(6) Schröder, C.; Rudas, T.; Steinhauser, O. *J. Chem. Phys.* **2006**, *125*, 244506.
(7) Kremer, F.; Schönhals, A. *Broadband Dielectric Spectroscopy*; Springer: Berlin, Germany, 2003.
(8) Kaatze, U.; Feldman, Y. *Meas. Sci. Technol.* **2006**, *17*, R17.
(9) Weingärtner, H. *Z. Phys. Chem.* **2006**, *220*, 1395.
(10) Daguenet, C.; Dyson, P. J.; Krossing, I.; Olleinikova, A.; Slattery, J.; Wakai, C.; Weingärtner, H. *J. Phys. Chem. B* **2006**, *110*, 12682.
(11) Schroeder, C.; Wakai, C.; Weingärtner, H.; Steinhauser, O. *J. Chem. Phys.* **2007**, *126*, 044505.
(12) Weingärtner, H.; Sasisanker, P.; Daguenet, C.; Dyson, P. J.; Krossing, I.; Olleinikova, A.; Slattery, J.; Schubert, T. *J. Phys. Chem. B* **2007**, *111*, 4775.
(13) Asaki, M. L. T.; Redondo, A.; Zawodzinski, T. A.; Taylor, A. J. *J. Chem. Phys.* **2002**, *116*, 10377.
(14) Yamamoto, K.; Tani, M.; Hangyo, M. *J. Phys. Chem. B* **2007**, *111*, 4854.
(15) Koeberg, M.; Wu, C.-C.; Kim, D.; Bonn, M. *Chem. Phys. Lett.* **2007**, *439*, 60.
(16) Schrödle, S.; Annat, G.; MacFarlane, D. R.; Forsyth, M.; Buchner, R.; Hefter, G. *Aust. J. Chem.* **2007**, *60*, 6.
(17) Halder, M.; Sanders Headley, L.; Mukherjee, P.; Song, X.; Petrich, J. W. *J. Phys. Chem. A* **2006**, *110*, 8623.
(18) Arzhantsev, S.; Jin, H.; Baker, G. A.; Maroncelli, M. *J. Phys. Chem. B* **2007**, *111*, 4978.
(19) Kobrak, M. N. *J. Chem. Phys.* **2007**, *127*, 184507.
(20) Horng, M. L.; Gardecki, J. A.; Papazyan, A.; Maroncelli, M. *J. Phys. Chem.* **1995**, *99*, 17311.
(21) Reference deleted in proof.
(22) Holbrey, J. D.; Seddon, K. R. *J. Chem. Soc., Dalton Trans.* **1999**, *13*, 2133.
(23) Fredlake, C. P.; Crosthwaite, J. M.; Hert, D. G.; Aki, S. N.; Brennecke, J. F. *J. Chem. Eng. Data* **2004**, *49*, 954.
(24) Buchner, R.; Barthel, J. *Ber. Bunsen-Ges. Phys. Chem.* **1997**, *101*, 1509.
(25) Buchner, R.; Hefter, G.; May, P. M. *J. Phys. Chem. A* **1999**, *103*, 1.
(26) Barthel, J.; Bachhuber, K.; Buchner, R.; Hetzenauer, H.; Kleebauer, M. *Ber. Bunsen-Ges. Phys. Chem.* **1991**, *95*, 853.
(27) Jepsen, P. U.; Fischer, B. M.; Thoman, A.; Helm, H.; Suh, J. Y.; Lopez, R.; Haglund, R. F., Jr. *Phys. Rev. B* **2006**, *74*, 205103.
(28) Fischer, B. M. Broadband THz Time-Domain Spectroscopy of Biomolecules. Ph.D. Thesis, Albrecht-Ludwigs-Universität, Freiburg, Germany, 2005.
(29) Schrödle, S.; Hefter, G.; Kunz, W.; Buchner, R. *Langmuir* **2006**, *22*, 924.
(30) Kumar, A. *J. Solution Chem.* **2008**, *37*, 203.
(31) Wagner, M.; Stanga, O.; Schroer, W. *Phys. Chem. Chem. Phys.* **2004**, *6*, 4421.
(32) Buchner, R.; Chen, T.; Hefter, G. *J. Phys. Chem. B* **2004**, *108*, 2365.
(33) Nishida, T.; Tashiro, Y.; Yamamoto, M. *J. Fluorine Chem.* **2003**, *120*, 135.
(34) Tokuda, H.; Tsuzuki, S.; Susan, M. A. B. H.; Hayamizu, K.; Watanabe, M. *J. Phys. Chem. B* **2006**, *110*, 19593.
(35) Sanmamed, Y. A.; Gonzalez-Salagado, D.; Troncoso, J.; Cerdeirina, C. A.; Romani, L. *Fluid Phase Equilib.* **2007**, *252*, 96.
(36) Van Valkenburg, M. E.; Vaughn, R. L.; Williams, M.; Wilkes, J. S. *Thermochim. Acta* **2005**, *425*, 181.
(37) Huddleston, J. G.; Visser, A. E.; Reichert, W. M.; Willauer, H. D.; Broker, G. A.; Rogers, R. D. *Green Chem.* **2001**, *3*, 156.
(38) Wang, J.; Zhu, A.; Zhuo, K. *J. Solution Chem.* **2005**, *34*, 585.
(39) Dzyuba, S. V.; Bartsch, R. A. *ChemPhysChem* **2002**, *3*, 161.
(40) Determined at 25 ± 1 °C with a CVO 120 high-resolution viscometer (Bohlin Instruments).
(41) Giraud, G.; Gordon, C. M.; Dunkin, I. R.; Wynne, K. *J. Chem. Phys.* **2003**, *119*, 464.
(42) Hyun, B.-R.; Dzyuba, S. V.; Bartsch, R. A.; Quitevis, E. L. *J. Phys. Chem. A* **2002**, *106*, 7579.
(43) Xiao, D.; Rajian, J. R.; Li, S.; Bartsch, R. A.; Quitevis, E. L. *J. Phys. Chem. B* **2006**, *110*, 16174.
(44) Xiao, D.; Rajian, J. R.; Cady, A.; Li, S.; Bartsch, R. A.; Quitevis, E. L. *J. Phys. Chem. B* **2007**, *111*, 4669.
(45) Wu, J.; Stark, J. P. W. *Meas. Sci. Technol.* **2006**, *17*, 781.